 SL, vol.6, no.2, pp.47-54, 2011

Implement and validation of Viscous Numerical Wave Flume Based on Finite Element Method and CLEAR-VOF Method

L. Lu[1] and B. Teng[2] and B. Chen[3]

Abstract: This work describes the numerical implements of a two-dimensional viscous Numerical Wave Flume (NWF), which is based on the Finite Element Method (FEM), Computational Lagrangian-Eulerian Advection Remap Volume of Fluid Method (CLEAR-VOF), internal wave generation and artificial wave damping. Owning to the inherent consistence of CLEAR-VOF with FEM, it allows the simulations to be conducted in the context of irregular mesh partition. The present numerical wave flume is validated by the problems of standing wave trains in front of vertical wall, liquid sloshing in container with multi-baffles, solitary wave propagation and diffusion over vertical step, wave-induced fluid resonance in narrow gaps.

Keywords: Numerical wave flume, N-S equation, Finite Element Method, CLEAR-VOF.

1 Introduction

Numerical simulations based on viscous fluid theory have become more and more popular in ocean engineering. One of the great achievements is the development of Viscous Numerical Wave Flume (VNWF) in two-dimensional space or the counterpart of 3-D Viscous Numerical Wave Tank (VNWT). These numerical models have been widely used in the field of wave action on and interaction with maritime structures, attributed to the fast development computer capacity and computational technique. The numerical simulations allow us to understand well the details of velocity field and pressure field, and the complicated physical phenomena behind, for example, the boundary layer separation, turbulent properties, vortex shedding and viscous damping. These problems remain difficulties in laboratory measure-

[1] CDE and SAIL, Dalian Univesity and Technology, Dalian, China
[2] SLCOE, Dalian University of Technology, Dalian, China
[3] School of Hydraulic Engineering, Dalian University of Technology, Dalian, China

ments and field observations. Nowadays, Computational Fluid Dynamics (CFD) is a powerful tool for the community of water wave mechanics.

The necessary components of a VNWF include (1) Navier-Stokes solver (2) free surface capture (3) wave generator and (4) wave absorber. The grid-based numerical methods developed so far are the Finite Difference Method (FDM), Finite Element Method (FEM) and the Finite Volume Method (FVM). The FDM requires the orthogonal rectangular meshes and hence has limitations for the problems involving complex boundary configurations. This restriction can be alleviated by using FVM, but the numerical accuracy is degraded. The FEM is free of the mesh topology, giving the great advantage over the FDM. In addition, considering the wide application of FEM in the structural analysis, it is desirable to develop VNWF (VNWT) in the frame of FEM for the purpose of investigating the coupled wave-structure interactions. However, the most popular interface capture technique of Volume of Fluid (VOF) method is originally designed for the FDM and inherently requires the regular mesh partition although other interface simulation techniques are available so far, for example, the cut-cell method, level-set method and moving grid method, etc. Therefore, the great challenge remained in the FEM-VOF based VNWF (VNWT) is the implementation of VOF with irregular mesh. This will be addressed in this article.

2 Numerical Implements

The fluid flow is assumed to be incompressible and homogeneous, the Navier-Stokes equations read,

$$\frac{\partial u_i}{\partial x_i} = \begin{cases} q(\mathbf{x},t) & \mathbf{x} \in \Omega_s \\ 0 & \mathbf{x} \notin \Omega_s \end{cases} \tag{1}$$

$$\frac{\partial u_i}{\partial t} + u_j \frac{\partial u_i}{\partial x_j} = -\frac{1}{\rho}\frac{\partial p}{\partial x_i} + \upsilon \frac{\partial}{\partial x_j}\left(\frac{\partial u_i}{\partial x_j}\right) + f_i + \frac{\upsilon}{3}\frac{\partial q}{\partial x_i} \tag{2}$$

where u_i is the velocity component in the i-*th* direction, t the time, p the pressure, ν the fluid viscosity, ρ the fluid density and f the body force. In Eq. (1), a source term q ($\mathbf{x}$, t) is introduced, which is activated in the source region $\Omega_{,s}$ for the wave generation, that is, the internal wave maker. Alternatively, the incident wave can also be generated by describing the velocities along the inlet boundary while forcing q ($\mathbf{x}$, t)$\equiv$ 0 throughout the computational domain.

For the linear monochromatic water waves the source function takes the form as follows,

$$q(t) = CH\sin(\omega t)/S \tag{3}$$

where C is the phase speed, H wave height, ω wave frequency and S the area of $\Omega_{,s}$.

In the present VNWF, artificial spongy layers are employed to reduce the reflected waves, where a damping force term is introduced into the body force of N-S equations, that is,

$$f_i = g_i + R_i \tag{4}$$

where g_i is the gravity acceleration (g_x=0, g_y= -9.81 m/s^2), R_i denotes the damping force,

$$R_y = -\lambda_y \cdot u_y = -k\left[(x - x_s)/D_p\right]^2 (y_b - y)/(y_b - y_h)u_y \tag{5}$$

where x_s is the coordinates of the start points of spongy layers, D_p is the total length of the damping zone, y_b and y_h are the elevations of the local seabed and free surface, respectively, and l_y is the damping coefficient. For the sake of numerical stability, R_x = 0 is adopted for the horizontal (wave traveling) direction.

When the reflected waves do not have significant disadvantages on the physical problem, the Sommerfeld-Olansky radiations condition is used along the outlet boundary,

$$\partial\Phi/\partial t + C_0 \cdot \partial\Phi/\partial \mathbf{n} = 0 \tag{6}$$

where Φ is used to denote the velocity, pressure and wave profile, C_0 is the local flow speed.

The governing equations are discretized by the three-step FEM (Jiang et al. 1993). The resulting linear system for velocity is solved by the lumped mass method and the Poisson-type pressure equation is solved by the preconditioned BI-CGSTAB method. For the detailed numerical discritization, it is referred to Lu et al. (2010).

In order to capture the free surface, the CLEAR-VOF method (Ashgriz et al., 2004) is adopted, which is inherently consistent with the FEM and the unstructured irregular computational meshes. As for the phase of fluid advection in CLEAR-VOF, the fluid bulk is moved in a Lagrangian sense based on a concept of fluid polygon,

$$\Delta\mathbf{x}^{\alpha} = \mathbf{u}_t^{\alpha}\Delta t \tag{7}$$

where $\Delta\mathbf{x}^{\alpha}$ is the displacement of vertex α of the fluid polygon, $\mathbf{u}_t^{\alpha}$ is the velocity vector of vertex α at the time instant t, Δt is the time step increment. The fractions of VOF in the computational mesh cells are obtained by the computational geometry operations for the intersection and overlapping of the moved fluid polygon and

the fixed background Eulerian meshes. As for the second phase of interface reconstruction, the Piece-wise Linear Interface Construction (PLIC) method is used. The free surface in an interface element is approximated by a line segment $g(\vec{x})$,

$$g(\vec{x}) = \vec{n} \cdot \vec{x} + b = 0 \tag{8}$$

where $\vec{n}$ is the local normal outward unit vector of the interface, evaluated by the local gradient of VOF function and b is a constant determined by an interactive procedure.

As far the water wave problem is concerned, it is desirable to neglect the viscous effects at the free surface and then a simple normal dynamic free surface boundary condition p = 0 can be imposed. However, the velocity boundary conditions on the interface have to be extrapolated from the internal fluid domain as suggested by Yang et al. (2006). At the solid wall, the non-slip boundary condition is applied, i.e., $\mathbf{u}$ = 0. The numerical simulations commonly starts from the still water state, which leads to the static water pressure and the flow velocity $\mathbf{u}$ ($\mathbf{x}$, 0) = 0.

3 Validation and application

3.1 Wave reflection against vertical wall

A linear water wave with amplitude A = 3 cm, period T = 1.57 s and wave length L = 3 m is generated by using the internal wave maker. The water depth is h = 0.5 m. The centre of source region is located at (-8 m, 0.38 m), occupying a rectangular area of 8 cm× 6 cm. The left boundary (x = -14 m) is set to be the solid wall, while Sommerfeld B.C is imposed at the right-end x = 1 m. The wave profiles during $20T \sim 21T$ with an interval of $T/30$ are shown in Fig. 1. It can be observed that the standing waves are well developed in the left half domain due to the wave reflection against the vertical wall. The standing waves have an amplitude of A = 6 cm, which is two times of the incident wave amplitude. The numerical results are in good agreement with the analytical solutions. It is confirmed that the reflected waves travel out of the right boundary without significant reflection, which indicates that the present Sommerfeld B.C. works well.

3.2 Water sloshing in partially filled container with baffles

A rectangular tank attached with two identical rigid thin baffles on the both vertical walls is forced to oscillate on the flat plane. The movement of tank follows,

$$\ddot{x}(t) = -x_0 \omega^2 \sin(\omega t) \tag{9}$$

where x_0=0.002 m and ω =5.29 rad/s, respectively. The tank width, liquid depth, baffle breadth and the distance between baffle and container bottom are 1.0 m,

0.5 m, 0.3 m and 0.35 m, respectively. We compared the time-series of the wave elevation ζ along the right wall from the present VNWF with those obtained by Biswal et al. (2006) using the non-linear potential flow model, as shown in Fig. 2.

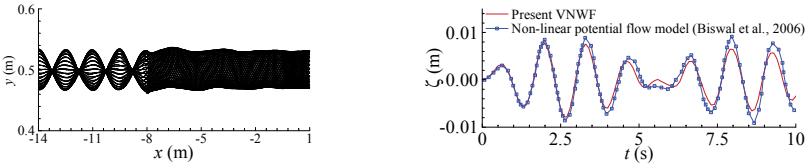

Figure 1: Linear wave reflection against wall ($20T \sim$21T, with interval T/30)

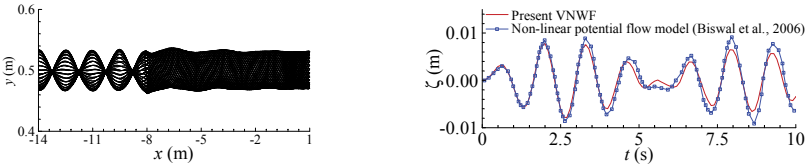

Figure 2: Comparison of wave elevations in oscillating container with baffles

It can be seen that the two sets of numerical results are generally in good agreement with each other. However, the wave amplitude from the potential model is found to be slightly greater than that of the present viscous model. This is because that potential flow model can not consider the energy dissipation due to the viscous damping and vortex shedding in this problem.

3.3 Solitary wave passing abrupt step

The soliton diffusion over abrupt step is simulated using the present VNWF. The water depth, step height are h = 0.2 m and d_s = 0.1 m, respectively. The solitary wave with an amplitude of A = 3.65 cm is generated by describing the velocity components along the inlet boundary, located at 4 m upstream of the step, as follows,

$$u = \varepsilon\sqrt{gh}\left\{\eta_* - \frac{1}{4}\varepsilon{\eta_*}^2 + \frac{1}{3}\frac{h^2}{C^2}\left[1 - \frac{3}{2}\left(\frac{y}{h}\right)^2\right]\frac{\partial^2\eta^*}{\partial t^2}\right\} \tag{10}$$

$$v = \varepsilon\sqrt{gh}\frac{z}{c}\left[\left(1 - \frac{1}{2}\varepsilon\eta^*\right)\frac{\partial\eta_*}{\partial t} + \frac{1}{3}\frac{h^2}{C^2}\left(1 - \frac{y^2}{2h^2}\right)\frac{\partial^3\eta^*}{\partial t^3}\right] \tag{11}$$

where $\varepsilon = A/h$, $\eta^* = \eta/A$ and η is the wave profile. At the outlet, the Sommerfeld boundary condition is imposed.

The numerical results are validated by comparing with experimental data (Seabra-Santos, et al. 1987) and numerical results (Liu and Cheng, 2001), as shown in Fig. 3 and Fig. 4.

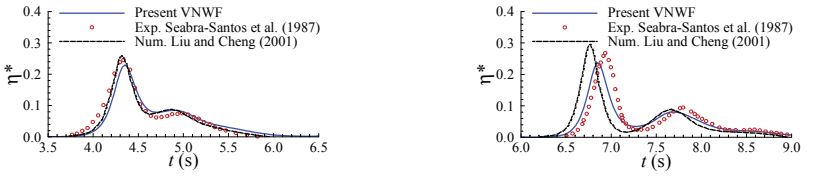

Figure 3: Wave profile evolution at 7 m downstream of step

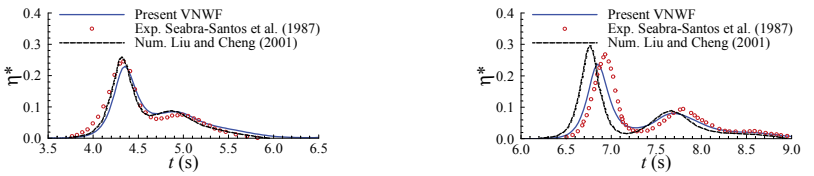

Figure 4: Wave profile evolution at 10 m downstream of step

Fig.3 and Fig. 4 illustrate that the present numerical results are generally in agreement with the previous experimental and numerical results. The soliton diffusion over shelf is simulated successfully. As for the position of 10 m (Fig. 4) some small discrepancies are observed. This is also reported by other researchers, for example, Shen and Chan (2010).

3.4 Fluid resonance in narrow gap formed by twin boxes

According to the laboratory tests (Saitoh et al., 2006), two identical boxes are fixed in a wave flume with water depth h = 0.5 m. The two boxes are arranged side-by-side leaving a small gap B_g = 11 cm in width between them. The breadth and draft of the twin bodies are B = 0.5 m and D = 0.155 m, respectively. In the numerical simulations, the internal wave maker is used to generate the target waves with amplitude of H = 2.4 cm covering a broad frequency band and the spongy layers are used to damping the reflected waves at the both ends of the computational

domain. The performance of spongy layer, for example, the left end under wave length L = 2m is shown in Fig. 5.

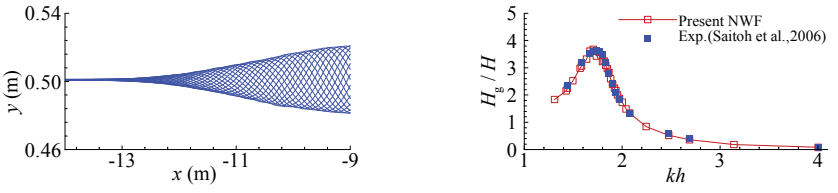

Figure 5: Reflected wave reducing in the left spongy layer (L= 2m, 49T $\sim$ 50 T)

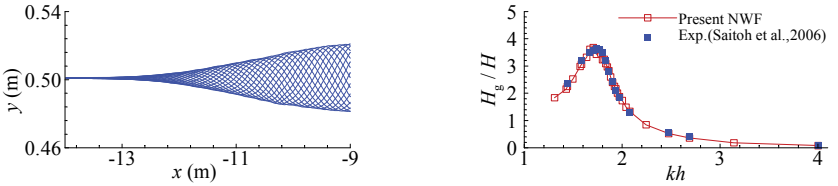

Figure 6: ariation of wave height in narrow gap with incident wave frequency

Some trivial numerical tests show that two times of the incident wave length of the damping zone together with the damping coefficient λ_y = 30 may lead to satisfying wave reduction. The numerical results of the variation of non-dimensional wave amplitudes in the narrow gaps (H_g/H) with incident wave frequency (kh, where k is the wave number) are compared with the experimental data, as shown in Fig. 6. It shows that the very large amplitude of wave oscillation in the narrow gap can be excited by the incident wave at the particular frequencies, that is, the resonant frequency. The numerical results of this work agree well with the experimental data (Saitoh et al., 2006). The resonant wave height in narrow gap is predicted accurately by the present VNWF, while it is over-estimated excessively by the conventional potential theory based model (Lu et al, 2010; Lu et al. 2011).

Acknowledgement: The authors gratefully acknowledge the financial supports from the Natural National Science Foundation of China (Grant Nos. 50909016, 50921001 and 10802014). This work was also partially supported by the Open Fund from the State Key Laboratory of Structural Analysis for Industrial Equipment (Grant No.GZ0909).

References

Ashgriz N., Barbat T., Wang G. (2004): A computational Lagrangian-Eulerian advection remap for free surface flows. *International Journal for Numerical Methods in Fluids*, vol. 44, pp. 1-32.

Biswal K. C., Bhattacharyya S. K. and Sinha P. K. (2006): Non-linear sloshing in partially liquid filled containers with baffles. *International Journal for Numerical Methods in Engineering*, vol. 68, pp. 317-337.

Jiang C. B. and Kawahara M. (1993): A three-step finite element method for unsteady incompressible flows. *Computational Mechanics*, vol. 11, pp, 355-370.

Lin P. Z., Liu P. L.-F. (1999): Internal wave maker for Navier-Stokes equations models. *Journal Waterway Port Coastal and Ocean Engineering*, vol. 125, no. 4, pp. 207-215.

Liu P. L-F and Cheng Y. G. (2001): A numerical study of the evolution of a solitary wave over a shelf. *Physics of Fluids*, vol.13, no. 6, pp. 1660-1667.

Lu L., Cheng L., Teng B. and Zhao M. (2010): Numerical investigation of fluid resonance in two narrow gaps of three identical rectangular structures. *Applied Ocean Research*, vol. 32, no. 2, pp. 177-190.

Lu L., Teng B., Cheng L., Sun L. and Chen X. B. (2011): Modelling of multibodies in close proximity under water waves — Fluid resonance in narrow gaps. *Science China Physics, Mechanics & Astronomy*, vol. 54, no. 1, pp. 16-25.

Saitoh T., Miao G. P. and Ishida H. (2006): Theoretical analysis on appearance condition of fluid resonance in a narrow gap between two modules of very large floating structure. *The 3rd Asia-Pacific Workshop on Marine Hydrodynamics, Shanghai, China,* pp 170-175.

Seabra-Santos F. L., Renouard D. P., Temperville A. M. (1987): Numerical and experimental study of the transformation of a solitary wave over a shelf or isolated obstacles. *Journal of Fluid Mechanics*, vol. 176, pp. 117-134.

Shen L. W., Chan E. S. (2010): Application of a combined IB-VOF model to wave-structure interactions. *Applied Ocean Research*, vol. 32, pp. 40-48.

Yang C., Löhner R. and Lu H. D. (2006): An unstructured-grid based volume-of-fluid method for extreme wave and freely-floating structure interactions. *Journal of Hydrodynamics Ser. B*, vol. 18, no. 3 (s1), pp. 415-422.